MULTIDISCIPLINARY SCIENCE JOURNAL

CONFERENCE PAPER
Published Online: August 10, 2023
https://doi.org/10.31893/multiscience.2023ss0112

Advancing Engineering, Science, and Technology: Innovations and Developments in Research and Development

The security of minimally invasive surgery with an autonomous flexible endoscope

Thiruvenkdam[a] | **Manish Kumar Goyal**[b] | **Vineet Saxena**[c]

[a]Jain (deemed to be) University, Bangalore, India, Associate Professor, Department of Computer Science and Information Technology.
[b]Vivekananda Global University, Jaipur, India, Assistant Professor, Department of Computer Science and Engineering.
[c]Teerthanker Mahaveer University, Moradabad, Uttar Pradesh, India, Assistant Professor, College Of Computing Science And Information Technology.

Abstract The surgical approach, Minimally Invasive Surgery (MIS), tries to limit stress on the patient's body and the number of incisions used during treatment. A flexible tube with a camera and light source known as an endoscope, which enables surgeons to see the interior organs and tissues, is one of the main instruments used in MIS. By expanding the capabilities of conventional endoscopes, Autonomous Flexible Endoscopes (AFE) can potentially change medical information systems. These autonomous devices can perform duties autonomously within the patient's body because they are outfitted with cutting-edge technology, including Artificial Intelligence (AI), computer vision, and robotic systems. Robotic surgical automation is a subject that is gaining more and more popularity. Although it is still impossible to fully automate a system, task and conditional autonomy are quite feasible. Safety is a key issue in robotic surgery, in addition to the performance of job completion. In this article, we introduce AFEs that can assist in autonomously guiding minimally invasive surgical procedures. The Tendon-driven Continuum Technique (TCT) served as the foundation for its development, and it is connected with the da Vinci Training Set (DVTS). There are six Degrees of Freedom (DOF) in the recommended AFEs. The surgical tools are automatically tracked using visual servoing. The AFE's mobility and space occupancy is minimized throughout the tracking process using an optimum control strategy, improving the safety of the robot system and any surrounding assistance. Both empirical and user research findings demonstrate that the suggested AFE has benefits over the current rigid endoscope in terms of safety and reduced space requirements without compromising comfort level.

Keywords: MIS, laparoscopy, surgical robotics, robot safety, visual tracking

1. Introduction

Patients today enjoy major benefits from shorter hospital stays, a lower risk of infection, and a general reduction in problems because of the development of MIS methods during the last several decades. Patients are also drawn to the aesthetic advancement of closed (laparotomic) operations because of the great decrease in scarring. Despite these advantages, MIS may cause extra difficulties for doctors by restricting the use of traditional instruments, preventing full visual and physical access to the operating room, and necessitating additional intensive training (Su et al 2021). The price of MIS rises as a result of these effects. The demand for many MIS treatments is still rising despite their expense to physicians and patients and their additional complexity. Transanal Endoscopic Microsurgery (TEM), compared to traditional transanal excision, improves resection quality, lowers the risk of local recurrence, and increases survival, especially in patients with early-stage rectal cancer with good histology. With comparable morbidity and mortality to traditional transanal excision, the technique of TEM excision of rectal cancers is safe and successful throughout long-term follow-up (Raucci et al 2020).

Although TEM has been in use for more than 20 years, colorectal surgeons have been sluggish to accept it as a standard procedure. This is partly due to a challenging learning curve, but it is also due to the exorbitant expense of the highly specialized apparatus. Technology is still developing quickly. The ability of the surgeon to do minimally invasive surgery has paralleled this development. Instrumentation created for one application may be applied to another via crossover. This is True of Natural Orifice Surgery (NOTES), carried out using TEM instruments and endoscopes (Runciman et al 2019). The Food and Drug Administration (FDA) approved the DVTS for several surgical procedures in 2000, including minimally invasive laparoscopic operations. Intuitive Surgical Company Inc., the DVTS, was developed and provides improved surgical dexterity, motion scaling, and tremor reduction. Sadly, da Vinci's stiff instruments restrict the available surgical entry sites in addition to the high price and huge size (Vo et al 2020).

The FDA has approved the da Vinci SP, a system created expressly for single port surgery, which will allow the da Vinci to be used in various emergent minimally invasive operations, even though these constraints have hampered the acceptance of this platform for usage in many procedures. Modern minimally invasive surgery has produced single-incision, multiport

devices that have made a variety of abdominal surgeries possible. Even single-access laparoscopy colectomies may now be done reliably and securely (Song et al 2020). Single-access laparoscopic working angles are almost equal to TEM working angles. Therefore, there is an overlap between the skill set required for TEM and single-port laparoscopy. However, a major obstacle to the widespread deployment of TEM apparatus continues to be its high initial cost. However, major advancements in the areas indicated above will be needed if a reliable surgical robotic system for these minimally invasive operations is to be realized. Robotic surgery will continue to be an expensive and time-consuming venture. It may struggle for years to gain widespread acceptance within the medical community if efforts are not made to better automate the robotic system and pair this with intuitive, simple-to-command user interfaces (Ma et al 2019). However, further advancements in autonomous robotic control can potentially enhance surgical results without significantly raising the price of these operations.

Surgery will be completely transformed by the thoughtful creation of partially autonomous MIS tools that support surgeons without the increased cost of several operators or much additional training. With its benefits of reduced pain, decreased risk of infection after surgery, and accelerated postoperative recovery, MIS has transformed conventional surgery (Huang et al 2022). In MIS, the endoscope is placed via a trocar to provide surgeons access to the body cavity. Endoscopes now in use have a robust and thin construction. These endoscopes provide several difficulties, including (1) exhausting the endoscope assistants; (2) requiring close coordination between the endoscope assistant and the surgeons; and (3) requiring a considerable motion area while rotating the rigid structure endoscope (Zhang et al 2021). Several solutions have been developed to deal with these problems. Many robotic endoscope-holding devices have been created to ease procedures, prevent surgeon fatigue, and minimize human mistakes (such as shaky hands while controlling the endoscope). To defend against possible cyber-attacks, preserve data confidentiality, and assure patient safety, AFE security is crucial in minimally invasive surgery (Slawinski et al 2018).

To determine the viability of prehabilitation in 22 women having breast cancer surgery, the research (Brahmbhatt 2020) performed a longitudinal, single-arm, mixed-methods study. For the course of their surgical wait period, each participant got a personalized exercise prescription that included strength and mobility training targeted to the upper quadrants as well as aerobic exercise. A detailed evaluation of some of the most prevalent force-torque sensor designs for surgical instruments was conducted in the study (Muscolo and Fiorini 2023), which also considered design and implementation restrictions. These constraints included those related to the robotic surgery environment, surgeon perception, general force-torque sensor design layouts, and force-torque sensors used in robot-assisted minimally invasive surgery. The transmission of surgical expertise is made easier with telementoring. The study (Shabir et al 2021) created a framework for telementoring that allows a specialized surgeon to guide an operating surgeon by imparting knowledge in the motion of surgical tools needed during minimally invasive surgery. An innovative force-sensing tool that supports teleoperated robotic manipulation and semi-automates the suturing process was introduced in the publication (Ehrampoosh et al 2022).

The end-effector mechanism features a rotating degree of freedom to construct the optimal needle insertion trajectory and pass the needle through its curve. An indirect force estimate method based on data-based models was employed to leverage impedance control to give the operator sensory knowledge of the forces between the needle and the tissue. The research (Su et al 2019) displayed whether redundancy is used to ensure a remote center of motion (RCM) restriction and to provide the medical personnel a compliant behavior. To complete the surgical tasks with human-robot interaction, an RCM constraint and a safe constraint are imposed on the nullspace motion based on the established hierarchical control architecture. The precision and safety of the procedure may be impacted by the physical contact. Robot-assisted minimally invasive surgery faces the basic but difficult challenge of automatic equipment separation in the video. By adding a derived temporal before an attention pyramid network for precise segmentation, the research (Jin et al 2019) provided a new framework for using instrument motion information. The inter-frame motion flow propagates the inferred prior from the previous frame to the current frame, which may provide a trustworthy indicator of the instrument placement and form.

The study (Lu et al 2023) offered a unique data-driven architecture with self-contained visual-shape fusion enabling flexible endoscopes to navigate autonomously and intelligently without the need for previous knowledge of system models or large-scale surroundings. The online updating of the eye-in-hand vision-motor arrangement and steering of the endoscope using monocular depth estimate through a vision transformer (ViT) is suggested using a learning-based adaptive visual servoing system. The path difficulty with the strategy (Pittiglio et al 2022) designed a magnetic interaction that would enable the catheter to adjust to the surrounding anatomy while in motion. They create and produce a soft magnetic catheter that is shape-forming, 80 mm long, and 2 mm in diameter. This catheter can follow the leader as it moves through the human body. The device might be used for various endoscopic or intravascular programs, but this study shows how well it works for navigational bronchoscopy.

The flexible endoscope that automatically follows the surgeon's head concerning the surgical target was suggested by the research (Qian et al 2020). by being operated on, the flexible robotic endoscope may see the surgical procedure from the surgeon's point of view. The endoscopic footage is seen by the surgeon while wearing a head-mounted display. The research (Mo et al 2022) described the creation of a novel workflow that, when combined with a flexible continuum robotic system,

offers task autonomy for laser-assisted surgery in confined areas like the GI tract. Contrary to the present, piezoelectric laser steering mechanisms demand the use of high voltage and are dangerous. The research Martin et al (2022) examined autonomous robotic control for magnetic colonoscope treatment through biopsy, another crucial aspect of clinical viability. They have created a variety of robotically autonomous control techniques, such as semi-autonomous routines for locating and carrying out focused and random quadrant biopsies. In this paper, we aim to explore the multifaceted security dimensions in this rapidly evolving field of MIS with an AFE.

2. Methodology

The safety of Minimally Invasive Surgery (MIS) using an Autonomous Flexible Endoscope (AFE) will be discussed in this section.

2.1. Autonomous Flexible Endoscopes (AFE)

The suggested AFE has six degrees of freedom (DOFs), with joints 1-4 of the Process Security Control (PSC) managing its insertion, pitch, roll, and yaw and joints 5 and 6 of the TCT controlling its bending. The TCT was able to bend in two orthogonal directions on its own. It is placed on a strong shaft that can move and rotate as well. Consequently, the final two connections of the flexible portion control the TCT, whereas the first four connections of the stiff segment of the suggested AFE are ordinary rigid connections. The dynamical framework for the 6-DOF flexible endoscopy is provided in the following sections.

A) The mechanics of a Rigid Component

The suggested AFE transition from distance set (set {0}) to set {4} corresponds to the PSC's transition from distance set (set {0}) to set {4} since TCT is mounted on the fourth set of the PSC (origin of set). Denavit-Hartenberg (D-H) technique may be used to calculate the rigid part's forward kinematics:

$$0_{S_4} = 0_{S_1} 1_{S_2} 2_{S_4} 3_{S_4} \qquad (1)$$

Where j_{S_i} the transition from is set {j} to set {i}, and $3_{S_4}, 2_{S_4}, 1_{S_2}, 0_{S_1}$ denotes the homogeneous translation matrices for the first, fourth, third, and second joints, correspondingly. The Jacobian matrix I_{rigid} for the rigid part presented below connects the speed of each joint of the rigid part $\dot{R}_{rigid}$ to direct kinematics.

$$0_{\dot{W}_4} = I_{rigid} \dot{Q}_{rigid} \qquad (2)$$

Where $0_{\dot{W}_4}$ denotes the set {4} reflected in distance set {0} velocity vector, composed of linear and angular velocities.

B) Dynamics of Flexible Component

On the fourth set of the PSC, the TCT is placed. As a result, set {4} provides the framework for the flexibility part of the planned AFE. Equation (3), provided at the bottom of this page, may be used to compute the matrix of homogeneous transformations from set 4 to the body set 4_{S_a} of the TCT. Here, θ denotes the flexible part's bending angle, Φ is the TCM's bending direction, and k denotes the flexible part's length. The following Jacobian matrix I_{flex} may be used to determine the linear and angular velocities associated with the flexible portion.

$$0_{S_1}\begin{bmatrix} cos^2\Phi(cos\theta - 1) + 1 & sin\Phi cos\Phi(cos\theta - 1) & cos\Phi sin\theta & \frac{1}{\theta}(1 - \cos(\theta))\cos(\Phi) \\ sin\Phi\ cos\Phi(cos\theta - 1) & cos^2\Phi(1 - cos\theta) + cos\theta & sin\Phi sin\theta & \frac{1}{\theta}(1 - \cos(\theta))\cos(\Phi) \\ -cos\Phi sin\theta & -sin\Phi sin\theta & cos\theta & \frac{1}{\theta}\sin(\theta) \\ 0 & 0 & 0 & 1 \end{bmatrix} \qquad (3)$$

$$I_{flex} = \begin{bmatrix} sin\Phi(cos\theta - 1)\frac{1}{\theta} & \frac{1}{\theta^2} cos\Phi(cos\theta + \theta sin\theta - 1) \\ -cos\Phi(cos\theta - 1)\frac{1}{\theta} & \frac{1}{\theta^2} sin\Phi(cos\theta + \theta sin\theta - 1) \\ 0 & -\frac{1}{\theta^2}(sin\theta - \theta cos\theta) \\ -cos\Phi sin\theta & -sin\Phi \\ -sin\Phi sin\theta & cos\Phi \\ 1 - cos\theta & 0 \end{bmatrix} \qquad (4)$$

The following diagram illustrates the joint speed of the flexible part:

$$4_{\dot{W}_a} = I_{flex} \dot{R}_{flex} \qquad (5)$$

Where $\dot{R}_{flex}$ is the joint velocity relative to the flexible component, the vector $4_{\dot{W}_a}$ for the body set {a} of the TCT shown in set {4} consists of the linear velocity and the rotation angle.

C) Mechanics of the 6-DOF AFEs

The frontal mechanic's version of the flexible endoscope with six DOF is illustrated below:

$$0_{S_d} = 0_{S_4} 4_{S_b} a_{S_d} = 0_{S_4} 4_{S_4} \qquad (6)$$

Where,

$$0_{S_d} = \begin{bmatrix} 1 & 0 & 0 & 0 \\ 0 & 1 & 0 & 0 \\ 0 & 0 & 1 & k_{ad} \\ 0 & 0 & 0 & 0 \end{bmatrix} \qquad (7)$$

is a continuous connection translation matrix going from camera set {d} to body set {b} of TCT. k_{ad}refers to the separation between the optical center of the endoscopy and the origin of the body set {b}. The 6-DOF flexible endoscope's end-effector speed may be calculated by

$$\dot{W} = I\dot{R} \qquad (8)$$

Where $\dot{R}$ denotes the speed of each AFE joint in the six degrees of freedom. The 6×6 Jacobian matrix provided below provides the speed map of a 6-DOF flexible endoscopy (I):

$$I = \left[I_{rigid} I_{rigid}\right] \qquad (9)$$

2.2. Vision Feedback

This section initially explains the suggested AFEs surgical tool tracking mechanism before introducing the visual servoing approach.

A) Tracking Method

The coordinates of the labels on the images must automatically follow the motions of surgical instruments in the suggested 6-DOF flexibility endoscope. The following are some challenges in tracking the surgical equipment: (1) The backdrop of the endoscopic pictures is rapidly shifting; (2) The instruments are rolling; and (3) the total amount of instruments is unknown.

Given that green is seldom seen naturally inside human bodies, it was decided to use it as the marker color in this work. The distal end of the surgical tools is marked with markers. The following is the tracking procedure: (1) initially, each RGB set green region is identified using the color-based picture segmentation technique. After completing the green area identification process, the RGB set is changed to grayscale and smoothed using a Gaussian filter. (2) Following that, corresponding areas that fall under a certain size threshold are removed from the image. To accommodate a variety of cameras, the threshold choice is made based on the dimensions of the source RGB image. (3) The center coordinates of all chosen related regions are then determined using the gray centroids approach. Figure 1 illustrates the proposed 6-DOF elastic endoscopy and is controlled by tracking points according to the average of these centered values.

B) Servo Visual Design

The relationship within the 2D data in images and the 3D data of the world is known as the camera system. The camera's 2D image measurements are transformed into 3D global coordinate data in the next section using there are two distinct types of coordinate schemes. In this study, the visualization concept is the pinhole method, which has the following equation as a formula:

$$Y_d \begin{bmatrix} v \\ u \\ 1 \end{bmatrix} = \begin{bmatrix} e/ox & 0 & v_0 & 0 \\ 0 & e/og & u_0 & 0 \\ 0 & 0 & 1 & 0 \end{bmatrix} \begin{bmatrix} w \\ z \\ y \\ 1 \end{bmatrix} \qquad (10)$$

Where (v_0, u_0)stands for the endoscope's image capture center coordinate, (v, u) for the retrieved image coordinates after the correction of image distortion, and $O = [w, z, y]^S$the referenced approach is used to fix the endoscope's distortion. The mobility of the suggested flexible endoscopy is then controlled using a cutting-edge 2D visual serving control technique (picture-based control).

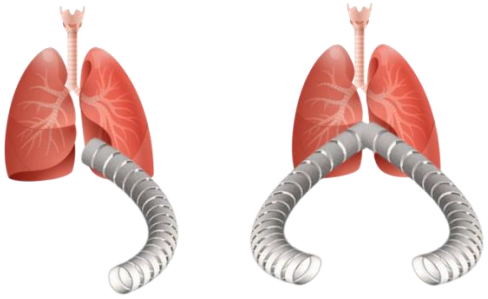

Figure 1 The tip of the surgical equipment is embellished with green markings.

$$\begin{bmatrix}\dot{v}\\ \dot{u}\end{bmatrix}=\begin{bmatrix}\frac{\lambda}{y} & 0 & -\frac{v}{y} & -\frac{vu}{\lambda} & \frac{\lambda^2+v^2}{\lambda} & -u\\ 0 & \frac{\lambda}{y} & -\frac{u}{y} & \frac{-\lambda^2-u^2}{\lambda} & \frac{vu}{\lambda} & -v\end{bmatrix}\begin{bmatrix}u_w\\ u_z\\ u_y\\ x_w\\ x_z\\ x_y\end{bmatrix}=\left[\frac{1}{y}G_U, G_X\right].W=\left[\frac{1}{y}\dot{G_U}, G_X\right].I.\dot{R} \quad (11)$$

Assume that the Jacobian variable y in the fixed camera system is unknown and that the end-effectors rotates with angular speed $[x_w, x_z, x_y]$ and translation velocity $[u_w,\ u_z, u_y]$ about the camera set. Therefore, to estimate the value of y online, we utilize observations of the robot and image motion. Using least-squares, it is possible to linearly extrapolate the value of y from equation (10).

2.3. Vision-Based Control Technique

This section begins with a proposal for optimum control with limitations on the minimum motion. The 6-DOF flexible endoscope's visual serving control loop is then presented.

A) The Best Control with the Least Movement

The penalty function is used in the optimal control method to optimize $R^l=(r_1^l, r_2^l, r_3^l, r_4^l, r_5^l, r_6^l)$. r_j^i represents the j-th joint's movement at time i. The minimal necessary border limitations are as follows:

$$r_1^l < r_1^{max} and\ r_2^l < r_2^{max} \quad (12)$$

The following penalty equation is created with restrictions (12):

$$e(R^l)=\alpha\left(\left\|r_1^l-r_1^{l-1}\right\|+\left\|r_2^l-r_2^{l-1}\right\|\right)+\beta\left(\left\|r_3^l-r_3^{l-1}\right\|+\left\|r_4^l-r_4^{l-1}\right\|+\left\|r_5^l-r_5^{l-1}\right\|+\left\|r_6^l-r_6^{l-1}\right\|\right)+q_1\min\{0, r_1^{max}-r_1^l\}^2+q_2\min\{0, r_2^{max}-r_2^l\}^2 \quad (13)$$

Where the safety factors q_1 and q_2 ensure that the values of r_1^l are less than $r_1^{max}$and q2, respectively. Weight factors α and β limit mobility in the first and second joints, respectively. Additionally, it is possible to calculate the variables$r_1^l, r_2^l, r_3^l, r_4^l, r_5^l$, and r_6^l by decreasing the objective function solution (14). Here, the optimization is carried out using the Levenberg-Marquardt method.

$$\text{minimize}\quad e(R^l)$$

$$subject\ to\begin{bmatrix}\dot{v}\\ \dot{u}\end{bmatrix}=\left[\frac{1}{y}G_U, G_X\right].I.\dot{R} \quad (14)$$

B) Control System for Instrument Tracking

The PSC is equipped with a designed flexible endoscope, which is computer-controlled. The general layout of the visual servoing control approach is shown in Figure 2.

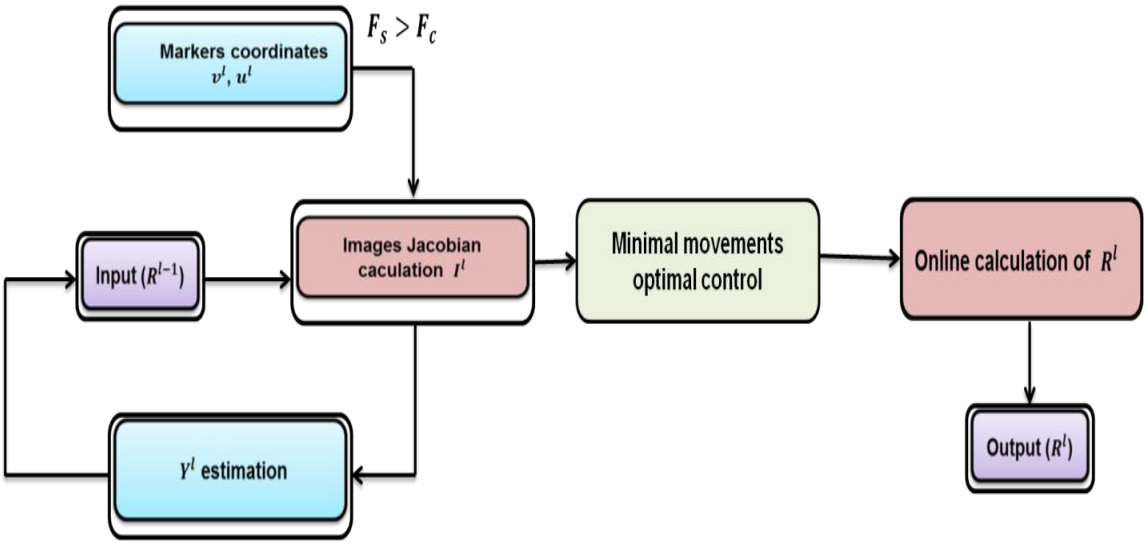

Figure 2 Control loop structure for monitoring inputs.

The endoscope obtains the image coordinate (v^l, u^l) of targets for the tracking structure, as shown in Figure 2. The monitoring fault F_s may then be determined by:

$$F_s = \sqrt{(v^l - v_c)^2 + (u^l - u_c)^2} \quad (15)$$

Fs represents the allowable error, and $(v_c, u_c)$for the target's intended image coordinate. Equation (10 may be used to estimate the image Jacobian $I^l$and the target's depth measurement if $F_s > F_d$is true. Following that, the motion of each joint R^lmay be reduced using the suggested optimum control approach. Last, processors will direct the actuators so that the flexible endoscope may move into the proper position and orientation.

3. Result and Discussion

The tracking abilities of both fixed and moving objects are examined in this segment. The recommended 6-DOF elastic endoscopy is then put to the test using the Fundamentals of Laparoscopic Surgery (FLS) exercises. Finally, user encounters with the rigid endoscopy and the recommended AFE are compared.

3.1. Experimental setup

The DVTS and a 6-DOF elastic endoscopy make up the test equipment. The DVTS controller operates the PSC. There are three parts to the flexible endoscope: (1) the distal end is equipped with a camera with a 640 x 480-pixel resolution that connects to a computer via USB. (2) A flexible bending portion comprises 10 vertebrae and an elastic foundation, with a set rate that may exceed 30 Hz. The flexible bending segment has an outside diameter of 7.5 mm and a length of 40 mm; it also has a rolling shaft from DVTS instrumentation and a mounting built by the user.

The calibration technique has been used to calibrate the endoscope, and Table 1 displays the endoscope variables. First-order radial distortion factor $l_1, l_2, o_1$and second-order radial distortion factor o_2 are, respectively, both the second-order radial compression ratio and the first-order radial compression ratio.

Table 1 Endoscope Specifications.

k_1	k_2	u_0	v_0	r_1	r_2	λ
0.0007	0.0013	3.18 pixels	244.9 pixels	0.0089	-0.18	810.3

3.2. Monitoring a Stationary Target

For In this section, the 6-DOF elastic endoscopy system tracks a stationary green marker on three occasions. The marker has a 3 mm diameter. The acceptable error value is 10

pixels F_s. The beginning location is on the bottom right edge, and the target graphic coordinate (v_c, u_c) is the picture's center coordinates (320, 240). Figure 3 displays the tracking trajectories from three iterations of the experiments. Results demonstrate the tracking's dependability.

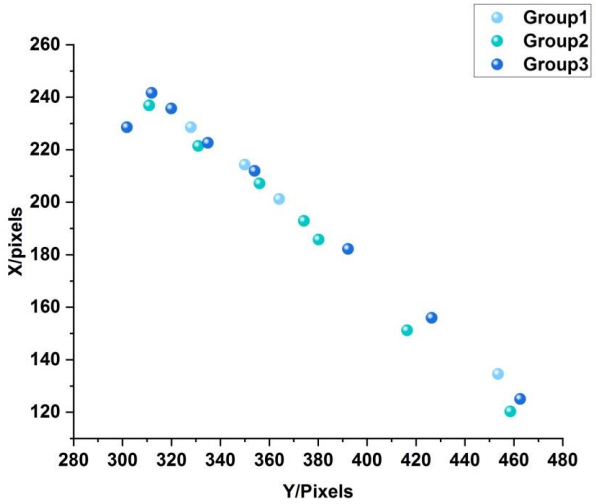

Figure 3 The graphic shows the target tracking trajectory. The target's intended location and beginning position on the image is shown by the pink symbols.

Figure 4 (a) displays the tracking error F_s for every convergence step. According to the color scores, the tracking error F_s value decreases to 10 pixels throughout 11 steps. The value of tracking error F_s during the first four steps falls quickly, from 270 pixels to less than 100 pixels.

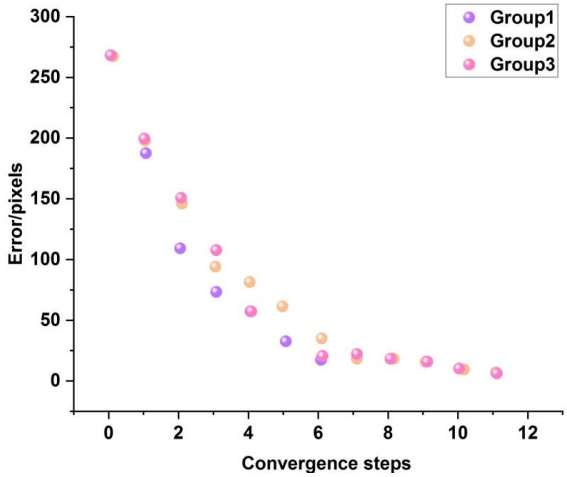

Figure 4 (a) Color points demonstrate that after 11 converging phases, the tracking error F_c value is reduced to 10 pixels.

Figure 4 (b) depicts the tracking time for each stage of convergence. After 1.71 seconds, the tracking error F_s will have decreased from 260 pixels to 10 pixels. Additionally, tracking speed is significantly influenced by the recommended AFE's motion ranges.

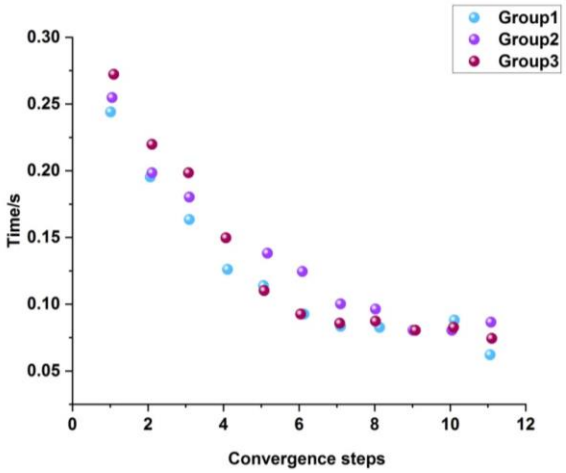

Figure 4 (b) The period of tracking at each resolution step of the tracking procedure is shown by colored spots.

There are five training assignments for the FLS manual skills. Some of these tasks include peg transfer, precision cutting, ligating loops, intracorporeal knotting, and extracorporeal knotting. To operate tools in a sufficiently wide area during the peg transfer, precision cutting, and extracorporeal knotting jobs, it is necessary to manipulate the endoscope to direct the work. To assess the effectiveness of the automated, flexible endoscope, three tasks, peg transfer, precise cutting, and extracorporeal knotting, are selected. Two flexible hand-held tools are used to operate the duties. The three jobs allow for good tracking of the two pieces of equipment. The three FLS tasks have also been required to be completed by 10 people using both the elastic endoscopic and the 4-DOF rigid endoscopic. The two endoscopes' comfort level is then scored (0–10 points). The results are shown in Figure 5. Table 2 displays the benefits of the suggested flexible endoscope.

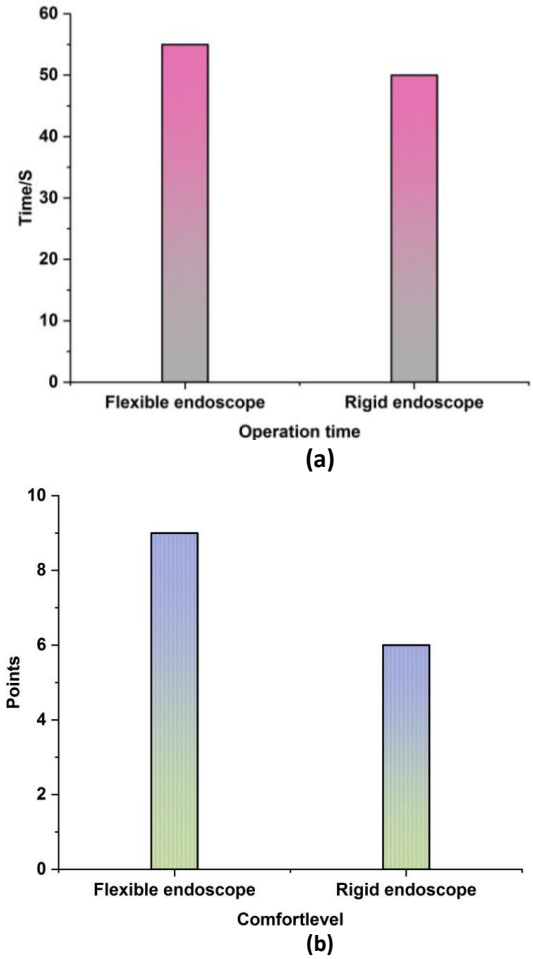

Figure 5 The contrast between the 4-DOF rigid endoscope and the suggested AFE. (a) The peg transfer's operating period. (b) The comfort level ratings.

Table 2 An evaluation of both flexible and rigid endoscopes.

	4-DOF Flexible endoscope	**6-DOF Rigid endoscope**
Operating	Average level	Average level
Motion space	Small	Large
Comfort level	Average level	Average level
Safety	good	Average level
Viewing field	Relatively large	Relatively small

From Figure 5, it is clear that the proposed AFE has much less interior and exterior occupied area than the 4-DOF rigid endoscope. This may improve the endoscopic method's safety during surgery and provide doctors access to more operating space. The results for task operation time and comfort level while using the two endoscopes that are pretty similar.

4. Conclusions

This study reports an autonomous 6-DOF flexible endoscopy with improved security. A distal bending segment of the suggested AFEs is based on the TCT. It has a total of six DOFs and is connected with the DVTS. It is possible to automatically track instruments using visual servoing. The endoscope movement is reduced during the instrument tracking procedure by using the best control approach. This lessens the risk of arms colliding outside the body and tools fencing within the surgical

cavity. The suggested AFE's performance is accessed via experimental testing. The suggested flexible endoscope can successfully monitor both fixed and moving objects, according to experimental data. This demonstrates how the suggested AFE might greatly decrease safety issues and save space during MIS treatments. Last, user research with 10 participants shown that the flexibility endoscopic may be used for MIS operations and that it could provide a wider field perspective and safer functioning than rigid endoscopes. The existing method has drawbacks, such as blurry images and uneven lighting within bodily cavities. Our ongoing research strives to lessen instrument-related picture blur. In addition, the suggested technology will eventually be integrated with stereoscopic 3D vision.

Ethical considerations

Not applicable.

Declaration of interest

The authors declare no conflicts of interest.

Funding

This research did not receive any financial support.

Reference

Brahmbhatt P, Sabiston CM, Lopez C, Chang E, Goodman J, Jones J, McCready D, Randall I, Rotstein S, Santa Mina D (2020) Feasibility of prehabilitation prior to breast cancer surgery: a mixed-methods study. Frontiers in Oncology 10:571091.

Ehrampoosh A, Shirinzadeh B, Pinskier J, Smith J, Moshinsky R, Zhong Y (2022) A force-feedback methodology for teleoperated suturing task in robotic-assisted minimally invasive surgery. Sensors 22:7829.

Huang Y, Li J, Zhang X, Xie K, Li J, Liu Y, Ng CSH, Chiu PWY, Li Z (2022) a surgeon preference-guided autonomous instrument tracking method with a robotic flexible endoscope based on dvrk platform. IEEE Robotics and Automation Letters 7:2250-2257.

Jin Y, Cheng K, Dou Q, Heng PA (2019) Incorporating temporal prior from motion flow for instrument segmentation in minimally invasive surgery video. In Medical Image Computing and Computer Assisted Intervention–MICCAI 2019: 22nd International Conference, Shenzhen, China, Proceedings, Part V 22, pp. 440-448. Springer International Publishing.

Lu Y, Wei R, Li B, Chen W, Zhou J, Dou Q, Sun D, Liu YH (2023) Autonomous Intelligent Navigation for Flexible Endoscopy Using Monocular Depth Guidance and 3-D Shape Planning. arXiv preprint arXiv:2302.13219.

Ma X, Song C, Chiu PW, Li Z (2019) Autonomous flexible endoscope for minimally invasive surgery with enhanced safety. IEEE Robotics and Automation Letters 4:2607-2613.

Martin JW, Barducci L, Scaglioni B, Norton JC, Winters C, Subramanian V, Arezzo A, Obstein KL, Valdastri P (2022) Robotic autonomy for magnetic endoscope biopsy. IEEE Transactions on Medical Robotics and Bionics 4:599-607.

Mo H, Li X, Ouyang B, Fang G, Jia Y (2022) Task Autonomy of a Flexible Endoscopic System for Laser-Assisted Surgery. Cyborg and Bionic Systems.

Muscolo GG, Fiorini P (2023) Force-Torque Sensors for Minimally Invasive Surgery Robotic Tools: An Overview. IEEE Transactions on Medical Robotics and Bionics.

Pittiglio G, loyd P, da Veiga T, Onaizah O, Pompili C, Chandler JH, Valdastri P (2022) Patient-specific magnetic catheters for atraumatic autonomous endoscopy. Soft Robotics 9:1120-1133.

Qian L, Song C, Jiang Y, Luo Q, Ma X, Chiu PW, Li Z, Kazanzides P (2020) January. FlexiVision: Teleporting the surgeon's eyes via robotic flexible endoscope and head-mounted display. In 2020 IEEE/RSJ International Conference on Intelligent Robots and Systems (IROS), pp. 3281-3287. IEEE.

Raucci, M.G., D'Amora, U., Ronca, A. and Ambrosio, L., 2020. Injectable functional biomaterials for minimally invasive surgery. Advanced healthcare materials 9:2000349.

Runciman M, Darzi A, Mylonas GP (2019) Soft robotics in minimally invasive surgery. Soft robotics 6:423-443.

Shabir D, Abdurahiman N, Padhan J, Trinh M, Balakrishnan S, Kurer M, Ali O, Al-Ansari A, Yaacoub E, Deng Z, Erbad A (2021) Towards development of a tele-mentoring framework for minimally invasive surgeries. The International Journal of Medical Robotics and Computer Assisted Surgery 17:e2305.

Slawinski PR, Taddese AZ, Musto KB, Sarker S, Valdastri P, Obstein KL (2018) Autonomously controlled magnetic flexible endoscope for colon exploration. Gastroenterology 154:1577-1579.

Song C, Ma X, Xia X, Chiu PWY, Chong CCN, Li Z (2020) A robotic flexible endoscope with shared autonomy: a study of mockup cholecystectomy. Surgical endoscopy 34:2730-2741.

Su H, Mariani A, Ovur SE, Menciassi A, Ferrigno G, De Momi E (2021) Toward teaching by demonstration for robot-assisted minimally invasive surgery. IEEE Transactions on Automation Science and Engineering 18:484-494.

Su H, Yang C, Ferrigno G, De Momi E (2019) Improved human–robot collaborative control of redundant robot for teleoperated minimally invasive surgery. IEEE Robotics and Automation Letters 4:447-1453.

Vo CD, Jiang B, Azad TD, Crawford NR, Bydon A, Theodore N (2020) Robotic spine surgery: current state in minimally invasive surgery. Global Spine Journal 10:34S-40S.

Zhang X, Li W, Ng WY, Huang Y, Xian Y, Chiu PWY, Li Z (2021). An autonomous robotic flexible endoscope system with a DNA-inspired continuum mechanism. In 2021 IEEE International Conference on Robotics and Automation (ICRA), pp. 12055-12060. IEEE.